STARS

University of Central Florida
STARS

Faculty Bibliography 1990s

Faculty Bibliography

1-1-1999

NSCAT normalized radar backscattering coefficient biases using homogenous land targets

Josko Zec
University of Central Florida

David G. Long

W. Linwood Jones
University of Central Florida

Find similar works at: https://stars.library.ucf.edu/facultybib1990
University of Central Florida Libraries http://library.ucf.edu

Recommended Citation

Zec, Josko; Long, David G.; and Jones, W. Linwood, "NSCAT normalized radar backscattering coefficient biases using homogenous land targets" (1999). *Faculty Bibliography 1990s*. 2913.
https://stars.library.ucf.edu/facultybib1990/2913

This Article is brought to you for free and open access by the Faculty Bibliography at STARS. It has been accepted for inclusion in Faculty Bibliography 1990s by an authorized administrator of STARS. For more information, please contact lee.dotson@ucf.edu.

University of Central Florida

STARS
Showcase of Text, Archives, Research & Scholarship

JOURNAL OF GEOPHYSICAL RESEARCH, VOL. 104, NO. C5, PAGES 11,557–11,568, MAY 15, 1999

NSCAT normalized radar backscattering coefficient biases using homogenous land targets

Josko Zec
Central Florida Remote Sensing Laboratory, Electrical and Computer Engineering Department, University of Central Florida, Orlando

David G. Long
Electrical and Computer Engineering Department, Brigham Young University, Provo, Utah

W. Linwood Jones
Central Florida Remote Sensing Laboratory, Electrical and Computer Engineering Department, University of Central Florida, Orlando

Abstract. The NASA scatterometer (NSCAT) is a spaceborne radar sensor designed to measure the normalized radar backscattering coefficient σ^0 of the Earth's surface. Over the ocean, backscatter measurements are used to infer surface wind vectors. Wind retrieval is based on a statistical relationship between short-ocean wave roughness (that causes the backscatter) and the surface wind speed and direction. For NSCAT geometry, multiple antennas are used to provide backscatter measurements at several azimuth directions to resolve wind direction ambiguities. To achieve the desired wind vector accuracy, these antenna beams must be calibrated within a few tenths of a decibel. A simple relative-calibration method is applied to the NASA scatterometer backscatter from homogenous, isotropic, large-area targets. These targets exhibit both azimuth and time invariant radar response. A simple polynomial model for incidence angle dependence of σ^0 is used, and the mean radar response from all antenna beams is taken as the reference. Corrections (σ^0 biases) are calculated as differences (in log space) between measurements from particular beam and the reference. This simple model is applied to data from the Amazon rain forest and the Siberian plain. These areas are tested for temporal stability within the calibration period (several weeks). High-resolution masks are applied to extract suitable calibration data sets. Calculated corrections for each antenna beam are added to NSCAT σ^0 measurements as a function of incidence angle. The magnitudes of corrections show the necessity of on-orbit calibration.

1. Introduction

Satellite scatterometers are spaceborne radars that are used to measure the normalized radar backscattering coefficient σ^0 of the Earth's surface illuminated by the antenna. Measuring σ^0 over the ocean enables retrieval of near-surface wind vectors. The physical basis for the retrieval is the empirical relation between radar backscatter and the small-scale sea surface roughness, known as the geophysical model function (GMF) [*Schroeder et al.*, 1982]. Surface roughness (caused by wind-induced waves) is related to the wind friction speed at the surface. Further, the spatial distribution of these waves is anisotropic; thus measuring σ^0 from different azimuths allows determination of the wind direction [*Naderi et al.*, 1991]. For satellite scatterometer configurations with nonarticulating antennas, separate antennas are needed to provide multiple-azimuth looks. Since relative changes in σ^0 (as a function of azimuth viewing) are used to infer the wind direction, it is very important that these antennas be well calibrated, at least in the relative sense. Desired relative calibration accuracy (of order 0.1 – 0.2 dB, which translates to as high as 10^0 retrieved wind direction error) requires postlaunch, on orbit calibration and verification. Absolute σ^0 biases that are common to all antenna beams contribute to biases in the inferred wind speed, but these may be removed once on orbit by "tuning" the GMF to match "surface truth" comparisons in the form of in situ wind observations and numerical weather model analyses.

For previous satellite-borne scatterometers, several postlaunch antenna beam balance methods have been used, namely, homogenous area targets, ground-based transponders, and global ocean surfaces. For the first method, potential targets must exhibit azimuth-independent and temporally stable radar response. At such calibration sites, equality is expected (between antenna beams) for all measurements taken at the same incidence angles [*Birer et al.*, 1982]. This method provides excellent relative normalization that is used to eliminate differences in σ^0 caused by absolute gain biases among antenna beams. An analysis of SeaSat A Scatterometer System (SASS) σ^0 data by *Kennet and Li* [1989] showed Amazon and Congo tropical rain forests to be homogenous over a large area. Detailed analysis of the SASS measured σ^0 over the Amazon showed some temporal and spatial variability that must be taken into account [*Birer et al.*, 1982]. To remove the effects of spatial variability, σ^0 data sets used for beam balancing can be filtered using a "mask" created by an enhancing scatterometer resolution algorithm developed by *Long et al.* [1993]. Results of this procedure are reported by *Long and Skouson* [1996] for the SASS σ^0 from the Amazon. Some diurnal variations in Amazon σ^0 measurements were observed in the past [*Birer et al.*, 1982; *Long and Skouson*, 1996]. This suggests sepa-

Copyright 1999 by the American Geophysical Union.

Paper number 1998JC900098.
0148-0227/99/1998JC900098$09.00

rating descending (daytime) from ascending (night) over flights for the NASA scatterometer (NSCAT) analysis.

In this paper we use this distributed land target technique to determine σ^0 biases for the NSCAT antennas. These results are compared to the ocean-derived antenna bias corrections ultimately applied to all NSCAT σ^0 [*Wentz and Smith*, this issue; *Freilich and Dunbar*, this issue]. After a brief introduction to the NSCAT instrument in the next section (a broader description is given by *Naderi et al.* [1991]), the beam calibration model is described. Calibration data sets are extracted using resolution-enhanced land masks. Potential calibration sites are tested for temporal stability within the data accumulation period. Results are presented for the Amazon rain forest (traditionally used) and the Siberian plain. Correction tables, derived for each beam, are used to achieve balanced σ^0 response over the NSCAT incidence angles.

2. NASA Scatterometer

Spaceborne scatterometers are expected to become a key source of near-surface ocean wind vector observations in the future. This is because of their demonstrated ability to provide all-weather frequent measurements with uniform global coverage. The Ku band NASA scatterometer is the latest satellite scatterometer following SkyLab (1973, Ku band), SeaSat A scatterometer (SASS, 1978, Ku band), and European Remote Sensing Satellite scatterometers (ERS 1 and 2, 1991 and 1996, C band). NSCAT was launched on August 17, 1996, on board Japan's Advanced Earth Observing Satellite (ADEOS). ADEOS failed on June 30, 1997, owing to solar panel malfunction; however, an extremely valuable set of ocean, ice, and land σ^0 measurements were obtained during its 9-month operation.

NSCAT transmits pulses at 14 GHz using six antennas that produce "fan beam" patterns on the Earth's surface as illustrated in Figure 1. These antennas are slotted waveguide-array-fed horns that produce fan beam patterns with beam widths of 25° (elevation) and 0.4° (azimuth). Fore beam (1 and 8) and aft beam (4 and 5) antennas are linear vertical polarization. The middle-azimuth antennas are dual-linear polarized, with beams 3 and 7 being horizontal and 2 and 6 vertical. This results in eight beams measuring σ^0 (four for each side; left side and right side swaths are independent). Prelaunch, the antennas are calibrated to within ± 0.25 dB using a cylindrical near-field antenna range at the Jet Propulsion Laboratory. On orbit, each antenna beam is sequentially illuminated, and the radar echo was subdivided into 25-km resolution σ^0 cells using Doppler processing [*Naderi et al.*, 1991]. This produces twenty-four, 25-km (along beam) by 7- to 11-km (cross beam), σ^0 resolution cells per beam. The corresponding incidence angle range is approximately 20° (near swath) to 60° (far swath).

NSCAT sequences through all eight beams during 3.74 s to achieve along-track beam sampling of 25 km, and after approximately 2 min, the fore and aft antenna samples fully overlap. With this configuration a surface location is sequentially viewed at three different azimuths as the satellite passes overhead. The σ^0 measurements taken in 25-km resolution cells are combined to produce wind vectors at 50-km resolution.

3. Calibration Model

Once on orbit, cross calibration between antennas must be performed to achieve maximum wind vector accuracy. Aircraft underflights proved inadequate during the SASS mission [*Birer et al.*, 1982]. Using homogenous land targets is a simple method producing accurate cross-calibration corrections in a relatively short time necessary to collect sufficient data quantity (typically 10 days). For any target, σ^0 is a function of location, time, azimuth, incidence angle, and polarization. Areas used for calibration must have isotropic radar response (i.e., be independent of azimuth [*Long and Skouson*, 1996]). Also, this response must be temporally stable over the period that the calibration data set is collected, and it must be uniform over a large area to eliminate location dependence. Further, targets should be nonpolarized such that they exhibit equal scattering characteristics for both vertical and horizontal polarization. Targets satisfying these criteria exhibit only incidence angle θ dependence in σ^0 response.

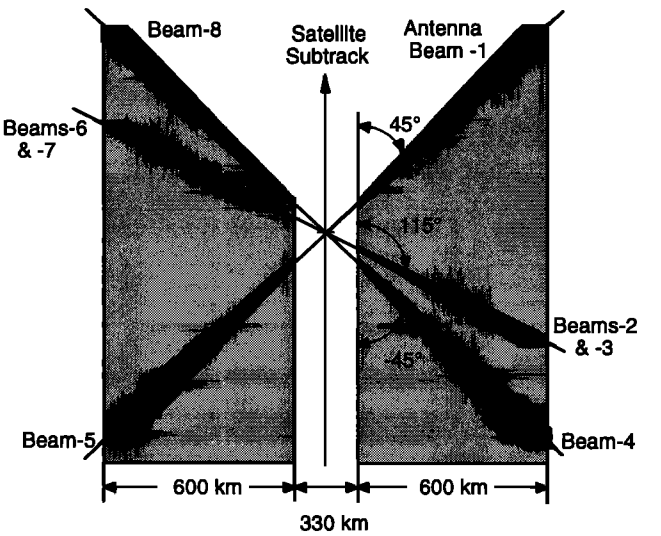

Figure 1. NASA scatterometer (NSCAT) antenna illumination patterns.

Calibration data sets are selected as discussed in section 4. Selected measurements are grouped into M smaller location elements. Following *Long and Skouson* [1996], a p order polynomial form is adopted as the model for the incidence angle response. Thus for beam i (i = 1 - 8) and location element l:

$$\hat{\sigma}^0_{i,l}(\theta) = a_{1,i,l} + a_{2,i,l}\theta + .. + a_{(p+1),i,l}\theta^p + \text{noise} \qquad (1)$$

$\hat{\sigma}^0{}_{i,l}(\theta)$ denotes modeled response calculated as the best fit in the mean square sense. It is calculated from instantaneous $\sigma^0(\theta)$ measurements falling completely within the element l. Regression analyses performed in linear (σ^0 ratio) and log (σ^0 dB) space yield very similar results, and linear regressions are used for the results presented herein. To calculate the a coefficients, a sufficient number of measurements must be collected to obtain stable estimates of the mean $\sigma^0(\theta)$ response. Typically, several thousand σ^0 are used for a given location element. The zero-mean noise term is due to random uncertainties in the radar equation parameters and communication noise (i.e., signal-to-noise effects). The noise term also includes some nonrandom effects such as rain backscatter/attenuation. ADEOS did not include an instrument for rain estimation, so that NSCAT σ^0 could be corrected for these effects. Nevertheless, a careful examination of the histograms of σ^0 demonstrates that the standard deviation was small (typically < 0.5 dB). Averaging responses from all beams (four

vertical and two horizontal), the reference set of polynomial coefficients $A_{k,l}$ becomes

$$A_{k,l} = \frac{1}{8}\sum_{i=1}^{8} a_{k,i,l} \qquad k=1....(p+1) \qquad (2)$$

resulting in the mean incidence angle response model

$$\overline{\sigma}^0_l(\theta) = \sum_{k=1}^{p+1} A_{k,l}\vartheta^{k-1} \qquad (3)$$

where $\vartheta = (\theta - 40^\circ)$ is taken for numerical stability near the beam boresight. A third-order polynomial fit model is tabulated in Table 1. Equation (2) combines both vertical and horizontal polarization (all beams). This approach is based on the observed polarization independence in Amazon σ^0 (θ) response [*Birer et al.*, 1982].

Averaging corrections from each location cell, the correction to be applied to beam i becomes

$$c_i(\theta) = 10\log_{10}\left\{\frac{1}{M}\sum_{l=1}^{M}\left[\frac{\overline{\sigma}^o{}_l(\theta)}{\overline{\sigma}^o{}_{i,l}(\theta)}\right]\right\} \qquad (4)$$

The corrections defined by (4) are added to raw σ^0 measurements to achieve equality among antennas. Applied corrections force individual beam responses to the reference value given by (3). This σ^0 correction method is easily applied and has been used previously [*Long and Skouson, 1996*].

NSCAT estimates the returned power P_s by subtracting a noise-only measurement P_n from the signal+noise measurement P_r, i.e. $P_s = P_r - P_n$. Since the measurements are noisy, estimates of P_s can be negative when the Signal-to-noise ratio (SNR) is low (i.e., when $P_r<P_n$), resulting in negative σ^0 measurements. Adding the bias correction as in (4) can scale the measurement errors since the bias correction is applied to the estimated σ^0. However, low SNR is not a concern over most land areas since σ^0 is typically larger than over the ocean. For example, the mean SNR for the data over the Amazon basin is ~8 dB and no cases of negative σ^0 were observed. Applying a bias correction that does not scale the measurement error is problematic since the measurements of P_r and P_n are noisy. However, given the magnitude of the corrections, applying the correction minimizes the σ^0 bias with only a very small effect on the measurement error statistics.

4. Calibration Data Sets

It is necessary to use data from areas with homogenous, isotropic, and nonpolarized radar response as calibration sets. Therefore careful data selection must be performed prior to incidence angle response modeling. Data are selected using masks produced using the scatterometer image reconstruction (SIR) algorithm [*Long et al.*, 1993]. SIR is a resolution enhancement algorithm based on spatial overlap of the measurements taken at nominal resolution during multiple passes (overflights). The algorithm uses first-order model for the incidence angle response:

$$\sigma^0 = A + B\theta \qquad (5)$$

where σ^0 is in decibels and $\vartheta = (\theta - 40^\circ)$. There A is the normalized radar cross section at 40° incidence angle and B is the incidence angle slope. To generate masks, location pixels with A response within ± 0.5 dB of the mean response of the area are selected for calibration [*Wilson*, 1998; *Long and Skouson*, 1996].

Table 1. Third Order Polynomial Model Coefficients of NSCAT $\sigma(\theta)$ Response over Amazon Tropical Rainforest

Coefficient	Value
A_1	0.207
A_2	-0.003
A_3	-0.00043
A_4	-0.0000013

Figure 2. Amazon mask used for data editing. Black pixels are within ± 0.5 dB of the mean normalized radar backscattering coefficient σ^o.

The Amazon rain forest mask for spatial data selection is shown in Figure 2. This region is a standard calibration target that has been used for SASS and ERS 1 calibration [*Long and Skouson*, 1996]. The river is clearly visible by following the excluded area (shown in white). Only those NSCAT σ^0 cells containing pixels that are completely within masks are included in the calibration data set.

To assure that the antenna beam σ^0 corrections (beam biases) are truly biases, it is desirable to perform calibrations at other locations. During the initial instrument calibration/validation activities, many other homogeneous regions were found [*Wilson*, 1998]; however, in this paper, we present σ^0 calibrations at just one of these. This is a large area with uniform A response in north central Russia (Siberia) as shown in Figure 3. Using exclusively masked data ensures spatial homogeneity of the target's response.

Long-term temporal stability is tested by dividing the σ^0 data into two nonoverlapping time series and computing averages. These 10-day time periods are November 6 -16 and 17 - 28, 1996. Plots of σ^0 versus incidence angle, hereafter called $\sigma^0(\theta)$, are shown in Figure 4 (Amazon) and Figure 5 (Siberia). From these data it is clear that the target responses are equal for both polarizations. This finding is consistent with those of previous investigators [*Birer et al.*, 1982]. For each beam, σ^0 (θ) is plotted for both time periods. Temporal stability is obvious, especially for the Amazon. For Siberia, minor σ^0 differences might be due to climatic (seasonal) changes at this higher latitude; nevertheless, they are small enough to qualify both targets as useful calibration sites. Increasing the amount of data, by extending the time window to about 3 weeks (20 days), could introduce seasonal effects into the radar response. Therefore a 3-week window is chosen as a compromise between the amount of data and time stability.

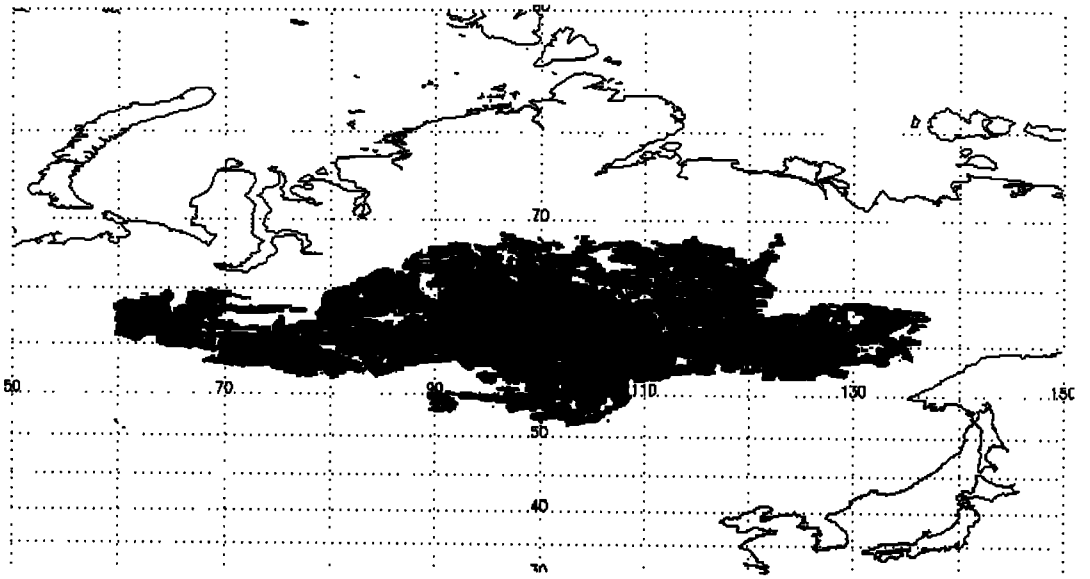

Figure 3. Siberian mask used for data editing. Black pixels are within ± 0.5 dB of the mean σ^o.

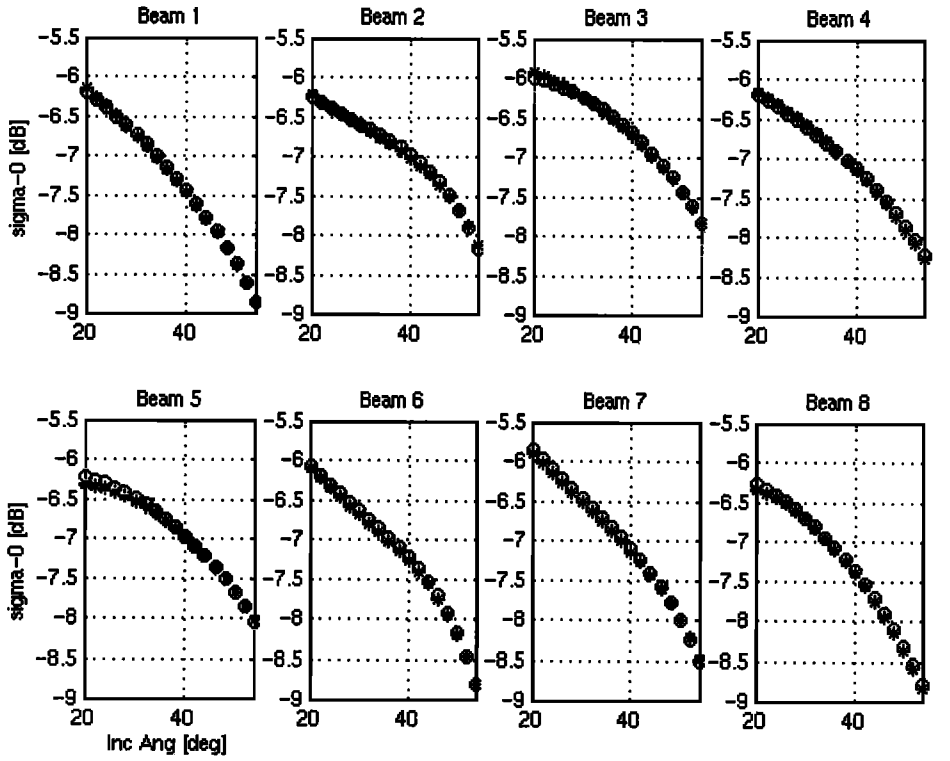

Period 1(Nov. 6. - Nov. 16.): *
Period 2 (Nov. 17. - Nov. 28.): o

Figure 4. Time stability of NSCAT $\sigma^0(\theta)$ response over Amazon for period 1, November 6 -16 (stars), and period 2, November 17-28 (circles).

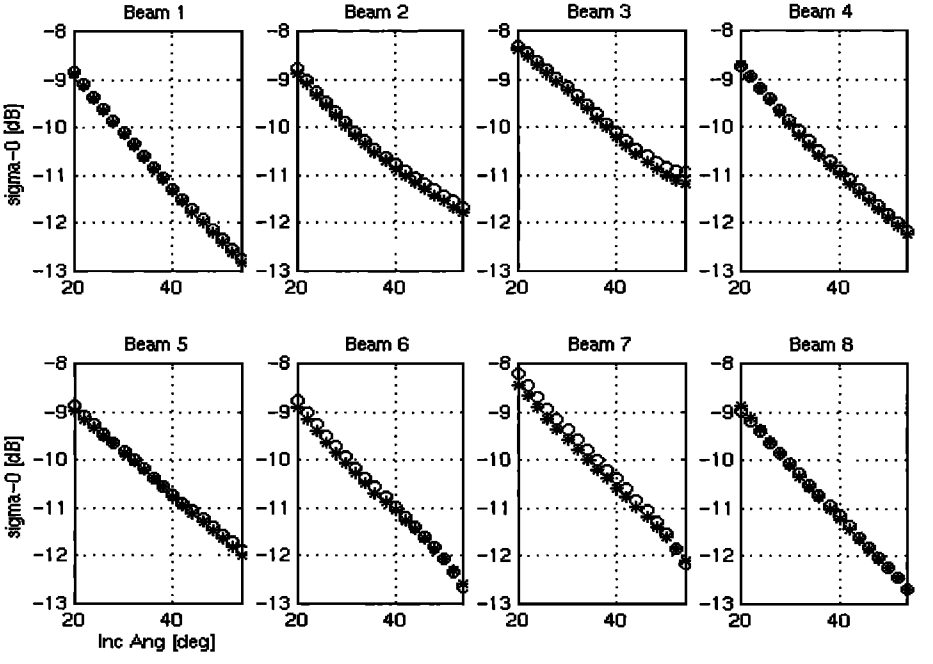

Figure 5. Time stability of NSCAT $\sigma^0(\theta)$ response over Siberia for period 1, November 6 -16 (stars), and period 2, November 17-28 (circles).

Besides seasonal effects there is a diurnal effect in the $\sigma^0(\theta)$ response for both regions. Previously, for both SASS and ERS 1, $\sigma^0(\theta)$ differences between night (ascending) and day (descending) passes have been observed [*Birer et al.*, 1982; *Long and Skouson*, 1996]. The geophysical causes for these diurnal differences are not completely understood. They have been attributed to morning dew on the forest leaves [*Birer et al.*, 1982] and to average orientation of leaves in the canopy at different Sun angles [*Long and Skouson*, 1996]. Since $\sigma^0(\theta)$ differs between spacecraft ascending and descending passes, the data set is separated according to the spacecraft direction. Therefore, during the NSCAT calibration period (November 6 - 28, 1996), separate ascending/descending $\sigma^0(\theta)$ responses are plotted for the Amazon basin in Figure 6. It should be noted that the calibration model is valid as long as the radar response is isotropic; thus changes in $\sigma^0(\theta)$ do not invalidate this technique. However, it is important that separate individual beam models (equation (1)) and reference model (equation (3)) be calculated for ascending and descending directions. Because the NSCAT antenna gains are expected to be time invariant, beam corrections (equation (4)) should be independent of the spacecraft direction. Comparisons between ascending and descending derived beam corrections will be discussed in section 5.

In previous investigations [*Birer et al.*, 1982; *Long and Skouson*, 1996], σ^0 data were used over the entire Amazon region. However, as explained in section 3, our calibration model divides the mask into M subset location elements. Dividing the Amazon mask into approximately semicircular elements of 500 km diameter results in M = 19 cells, which are depicted in Figure 7. This approach further strengthens the spatial homogeneity assumption because of the limited area over which measurements are grouped. Beam biases determined over smaller elements are averaged over the entire mask region. To assess the homogeneity of the Amazon mask, σ^0 biases were also determined using the entire mask and comparisons were made with the average of the elements. Results were very similar and differed by only several hundredths of a decibel. This is not considered to be statistically significant; therefore this result supports the approach taken by previous investigators.

5. Results

As described in the previous section, the calibration model is used on the selected data set. This model causes all beams to have the same $\sigma^0(\theta)$ response. The beam corrections (equation (4)) are applied to raw σ^0 measurements to obtain the mean $\overline{\sigma^0}(\theta)$ response (equation (3)).

Beam correction results, $c_i(\theta)$, shown in Figures 8 – 13 are close, but there are small differences that are statistically significant. For example, consider differences between ascending (night) and descending (day) $c_i(\theta)$ for the Amazon during the November 1996 window shown in Figure 8. For the right-hand swath (beams 1-4), the middle beams and the aft beam (2, 3, and 4) differ by less than 0.2 dB, essentially independent of incidence angle. On the other hand, the forward beam (1) exhibits an approximately parabolic dependence of the ascending/descending difference. For the left-hand swath (beams 5-8), the two middle beams that are mechanically connected appear to be offset by a constant 0.2 dB. This behavior is perplexing, in that it implies that the square of the peak gain for antenna beam 6 changes by 0.2 dB from the ascending (night) to descending (day) side of the orbit (σ^0 is proportional to antenna gain squared). The aft beam (5) appears to have a similar incidence angle characteristic as does the forward beam for the opposite side. A number of possi-

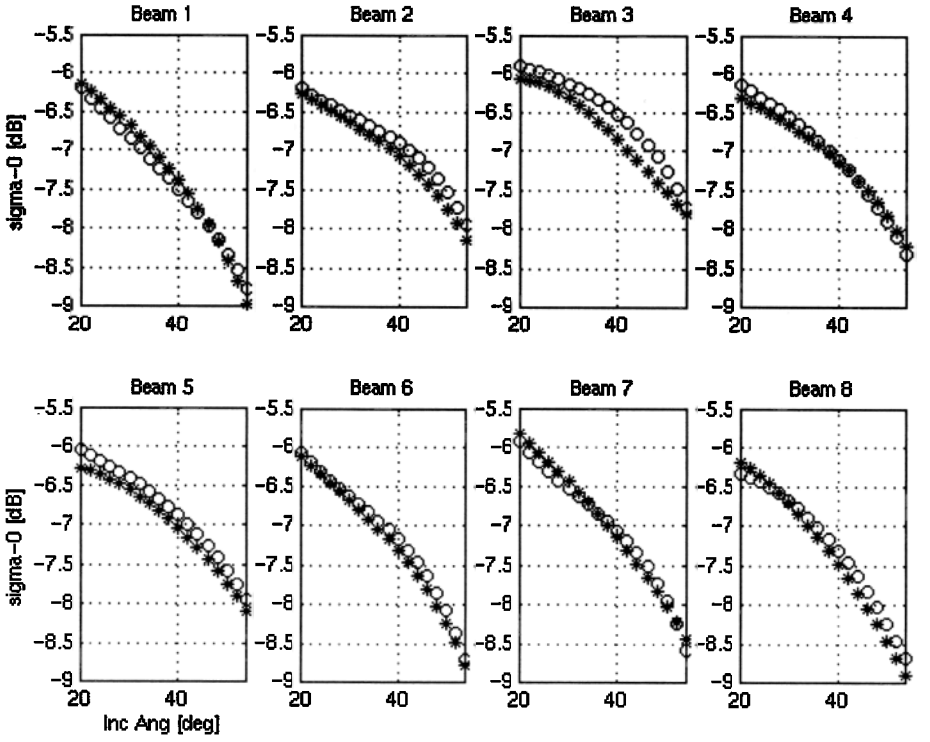

Figure 6. Diurnal effect of NSCAT $\sigma^0(\theta)$ response over Amazon for ascending passes (stars) and descending passes (circles).

ble causes to explain this behavior have been examined and dismissed; however, there is one that could explain most of the ascending/descending observations. We believe that the antenna bore sight is changing by several tenths of a degree during the orbit owing to unknown latitude-dependent offsets in the spacecraft attitude (roll, pitch, and yaw) [*Wilson*, 1998]. An independent spacecraft attitude investigation was conducted using ADEOS engineering data (J. A. Hashmall et al., private communication, 1997). Preliminary results support this hypothesis; but because the ADEOS housekeeping data are limited to only one orbit every

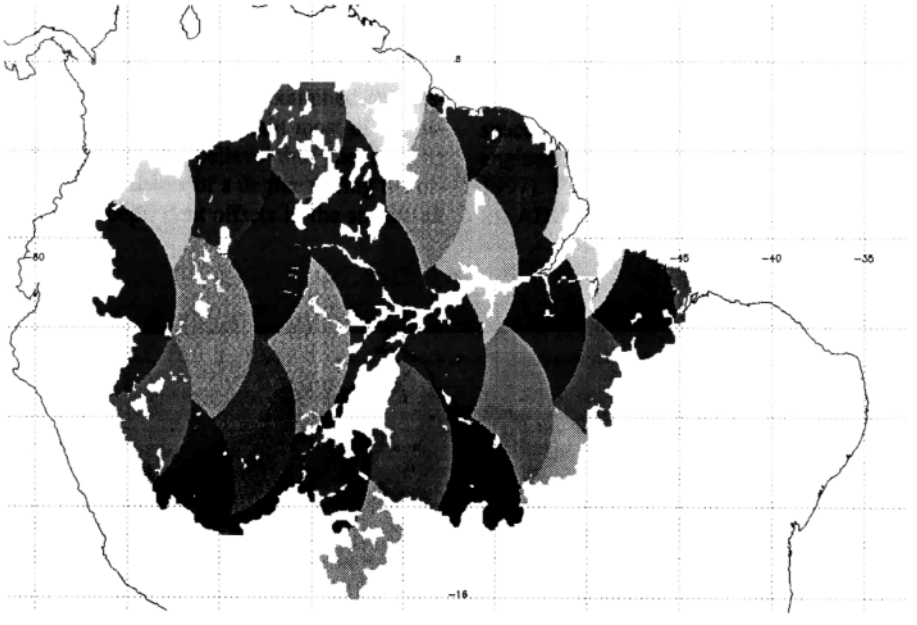

Figure 7. Boundaries of individual isotropic location elements.

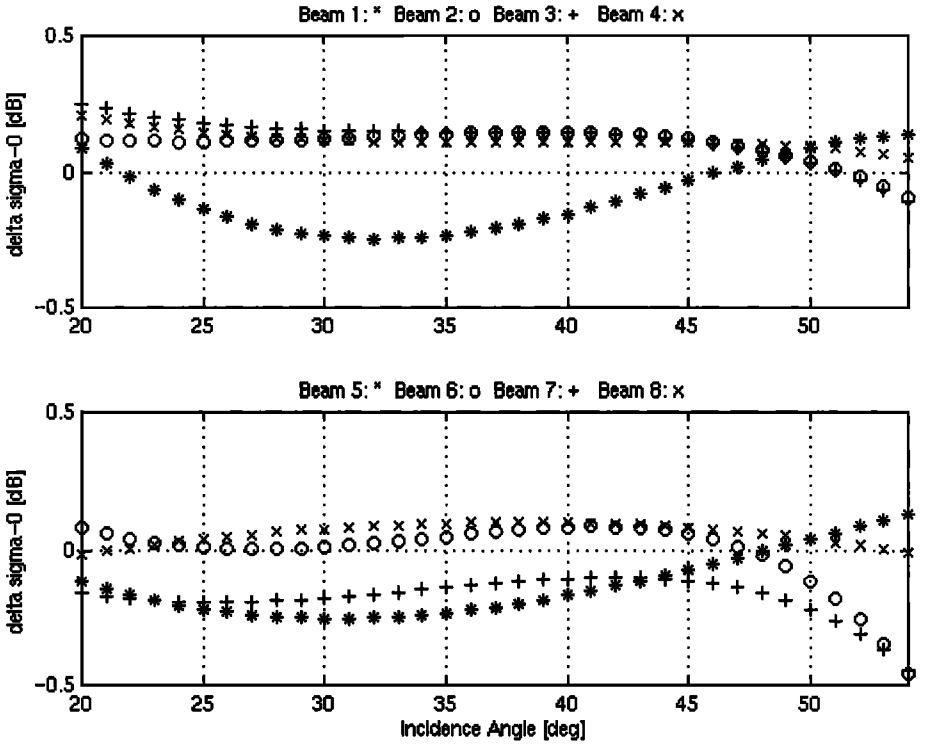

Figure 8. Differential beam corrections (ascending – descending revolutions) for Amazon, November 1996.

12 hours, the findings are not conclusive. Regardless, since the antenna gains are expected to be constant, the averages of the ascending and descending beam corrections are used.

Figure 9 shows calculated (average of ascending and descending) $c_i(\theta)$ for the Amazon during November 1996. Again, plots are separated for the right- and left-hand swaths. The individual beam corrections are of the order of few tenths of a decibel, which is significant for desired wind vector accuracy. Collectively, all beams are within ±0.5 dB. Recognizing that the antenna gain enters into the radar equation (σ^0 calculation) as a squared parameter, these results compare favorably with the prelaunch, near-field antenna gain calibration accuracy of ±0.25 dB.

Figure 10 shows the same $c_i(\theta)$ plots for the Siberian region for November 1996. For corresponding beams, similar curves are noted in Figures 9 and 10; however, there are some differences of

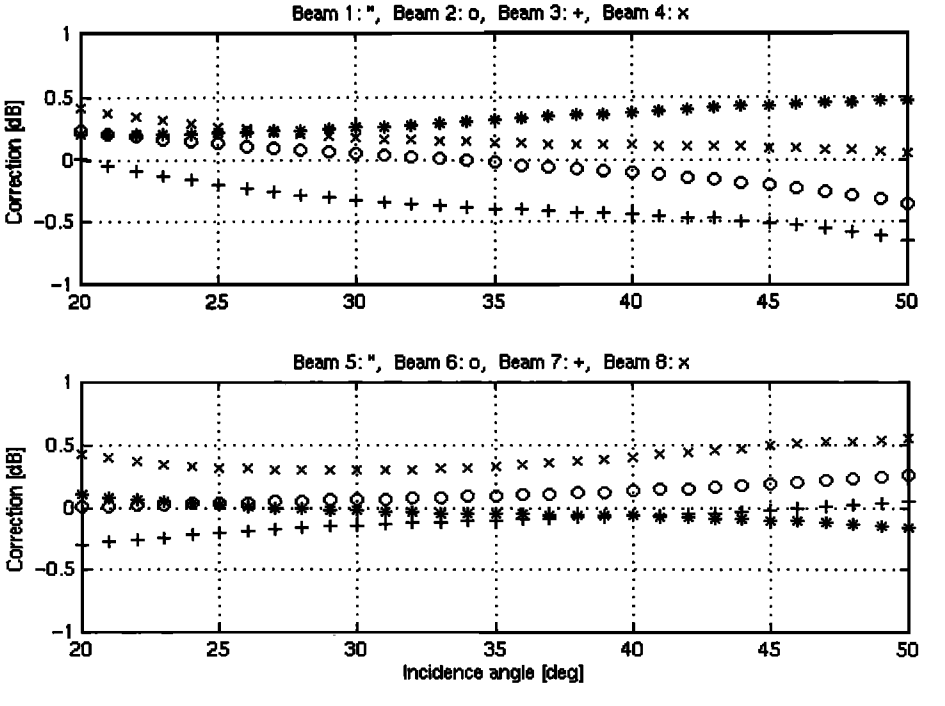

Figure 9. Beam corrections based on Amazon November 1996 data.

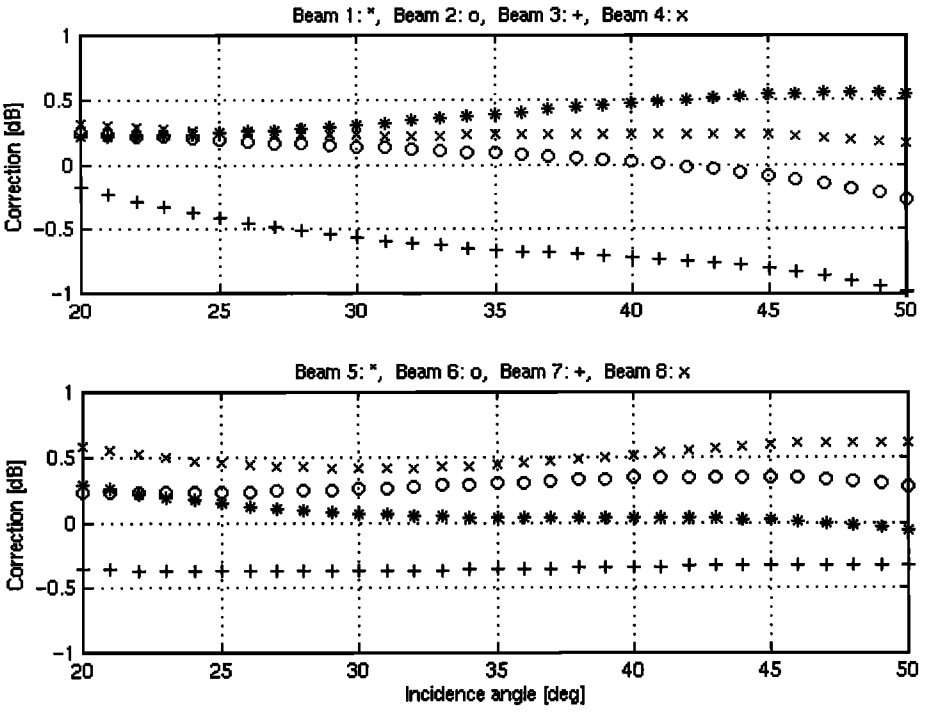

Figure 10. Beam corrections based on Siberia November 1996 data.

a few tenths of a decibel. These differences are highest for horizontally polarized beams 3 and 7, suggesting possible polarization effects. However, even these extreme differences are within projected calibration accuracy. Because of the excellent stability of the NSCAT instrument, the observed repeatability of the mean Amazon σ^0 (θ) for 10-day periods has a standard deviation of about 0.02–0.04 dB. For Siberia, the repeatability is less good, but generally within a factor of 2 (i.e., about 0.04–0.08 dB). Beam biases should be independent of the data set; thus good agreement between Amazon and Siberia is expected. Yet there are observed σ^0 (θ) differences of a few tenths of a dB; they cannot be explained by statistical uncertainty. Some difference in the beam corrections could be attributed to changes in the Siberia σ^0 (θ) due to more severe weather changes. Another possibility is variability of the antenna bore sight with latitude (discussed in the preceding paragraph). Regardless of the cause, because of the

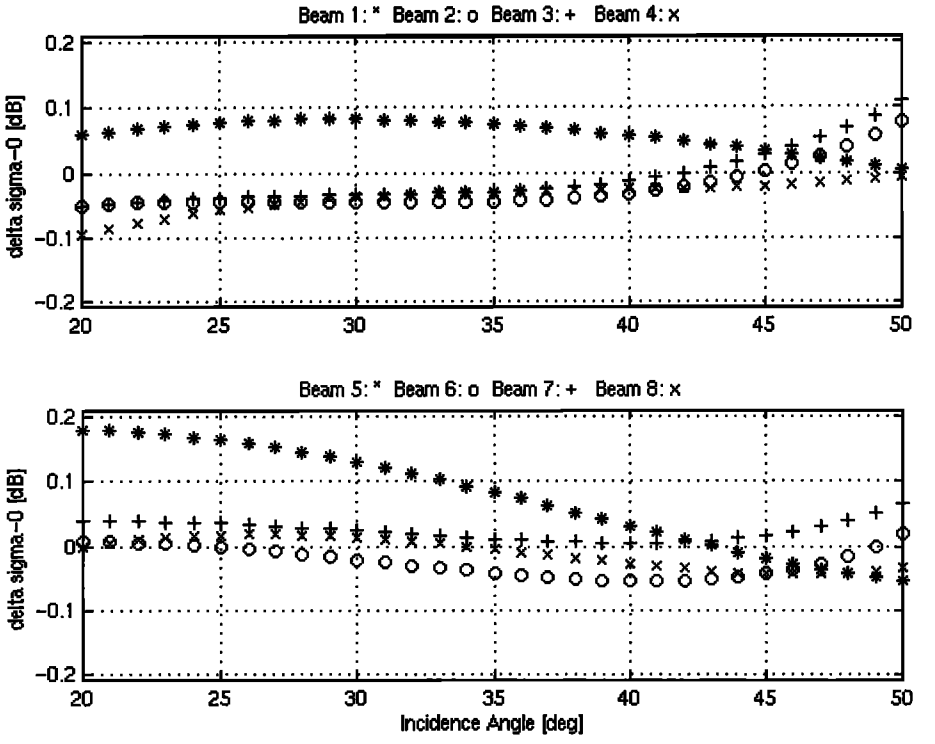

Figure 11. Differential beam corrections (November 96 - January 1997) from Amazon data.

greater confidence in the Amazon data, it is used for calibration purposes. Nevertheless, the Siberian data are still useful to provide independent confirmation of the beam bias stability.

Confidence in the beam bias stability is also gained by repeating calibration for a different time period. For the Amazon the excellent stability of the beam biases is observed (in Figure 11) by calculating differences between the corresponding beam corrections derived from two time periods: November 6 - 28, 1996, and January 8 – 29, 1997. For the right-hand swath, beams 2, 3, and 4 differ by less than 0.05 dB for most incidence angles. Only near the extremes of the incidence angles do the deltas increase to about 0.1 dB. This is most likely the result of the less accurate regression fit due to the reduced number of σ^0 at these incidence angles. Even though the forward beam exhibits the worst behavior, it is still excellent (delta less than 0.1 dB). For the left-hand swath, beam biases exhibit slightly less accurate results. Only beam 5 exceeds deltas of greater than 0.1 dB and then only for incidence angles below 33°; all deltas are less than 0.2 dB. The curves for beams 1 and 5 are different from those of the other beams; however, these differences are not significant and are within desired calibration accuracy (≈0.2 dB). These results demonstrate that beam corrections are extremely stable and that residual error after compensation should be less than about 0.1 dB. This will produce negligible biases in the retrieved ocean surface wind vectors.

The corresponding results for Siberia (Figure 12) are similar. Here changes in the beam biases, estimated from data taken over Siberia in two time periods: November 6 - 28, 1996, and January 8 - 29, 1997, are presented. The curve shapes for particular beams differ somewhat from the Amazon-based curves in Figure 11. This should be attributed to more severe seasonal changes of the Siberian radar response. However, even for a less time-stable target, such as Siberia, the derived NSCAT beam biases are still consistent within ± 0.2 dB.

The effect of correcting σ^0 measurements by application of beam corrections is illustrated in Figure 13, where separate $\sigma^0(\theta)$ responses for ascending and descending spacecraft direction are given. Raw (uncorrected) σ^0 measurements show significant scatter among individual beam responses that illustrate the need for beam balancing. Applying the averaged (ascending and descending) beam corrections significantly reduces this scatter (i.e., reduces standard deviation of measurements). Note that the $\sigma^0(\theta)$ response converges for all antenna beams at an incidence angle near the beam bore sights (about 47° where the antenna gain varies slowly with angle). For incidence angles removed from this bore sight, the σ^0 differences between beams grow larger with increasing (and decreasing) incidence angle. This suggests that there may be small pointing errors among beams and that slight pointing adjustments could improve the agreement. Since NSCAT utilizes Doppler processing to form σ^0 cells (incidence angles), pointing to each cell is related to Doppler frequency shift rather than just geometric angle. Because of this, each beam requires a different bore sight adjustment. Simulations performed to assess this effect, show that, for the worst case beam, adjustments of order 0.5° are required to improve the agreement over the given incidence angle range. A subsequent analysis of antenna deployment errors and thermal-induced alignment distortions cannot account for even 0.1° error; so we believe that spacecraft attitude offsets for ascending and descending portions of the orbit may be the cause.

Thus, while applying the average beam corrections is imperfect, it provides excellent beam balance for the ocean wind vector measurement application. Further, since the "true" value of σ^0 is not known, adjusting the measurements to the average results in a relative calibration that makes σ^0 measurements consistent among themselves rather than an absolute σ^0. Any residual absolute biases may be removed by adjustments in the geophysical model

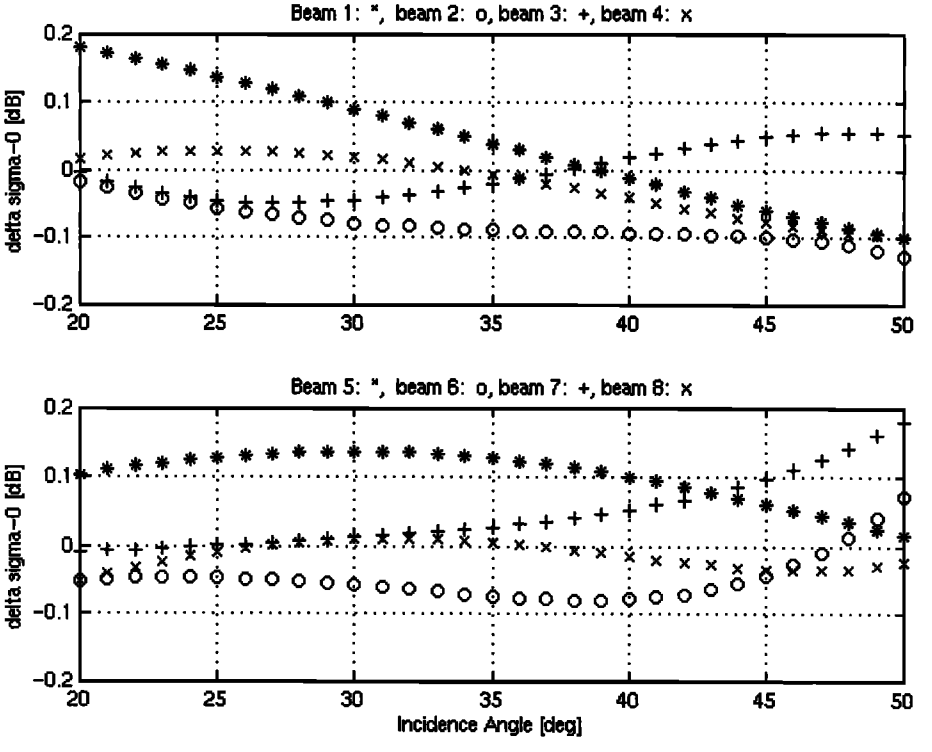

Figure 12. Differential beam corrections (November 96 - January 1997) from Siberian data.

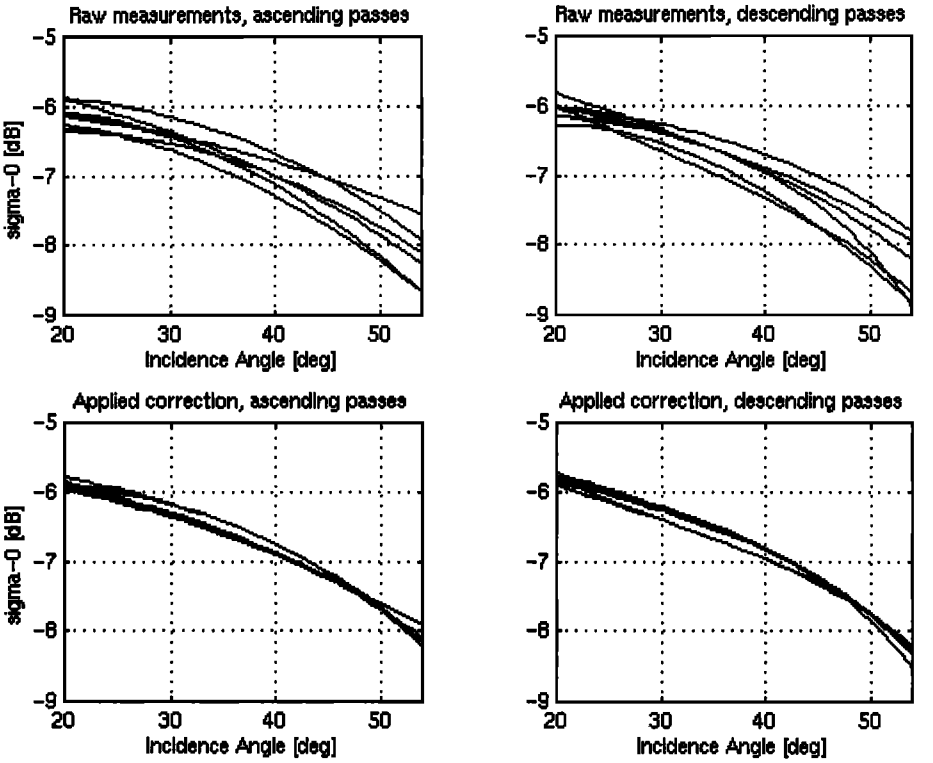

Figure 13. Effects of corrections on beam response for Amazon, November 1996.

function during on-orbit geophysical validation with surface truth.

During NSCAT postlaunch calibration, beam biases were also determined using alternative analyzes of the ocean backscatter. These techniques developed by *Wentz and Smith* [this issue] and *Freilich and Dunbar* [this issue] were judged (by the NSCAT engineering team) to best represent the biases for the ocean σ^0 measurement. These techniques were based on comparisons with ocean wind field models provided by the National Weather Service and the European Centre for Medium-Range Weather Forecasting. Beam balance was determined by adjusting σ^0 so as to retrieve (using the GMF) winds that were in the closest agreement with the numerical weather models. Thus this method critically depends on the accuracy of both GMF and referent wind model. Any inaccuracy in either of the two would produce erroneous σ^0 bias estimations. Thus erroneous σ^0 could retrieve cor-

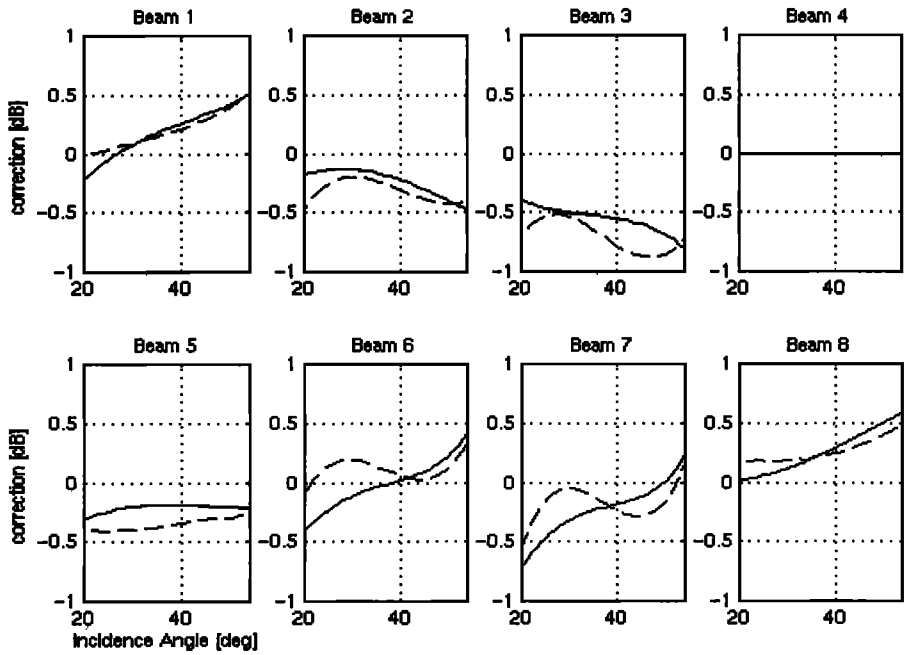

Figure 14. Comparison of NSCAT baseline, ocean-derived, and land-derived beam corrections for ascending passes.

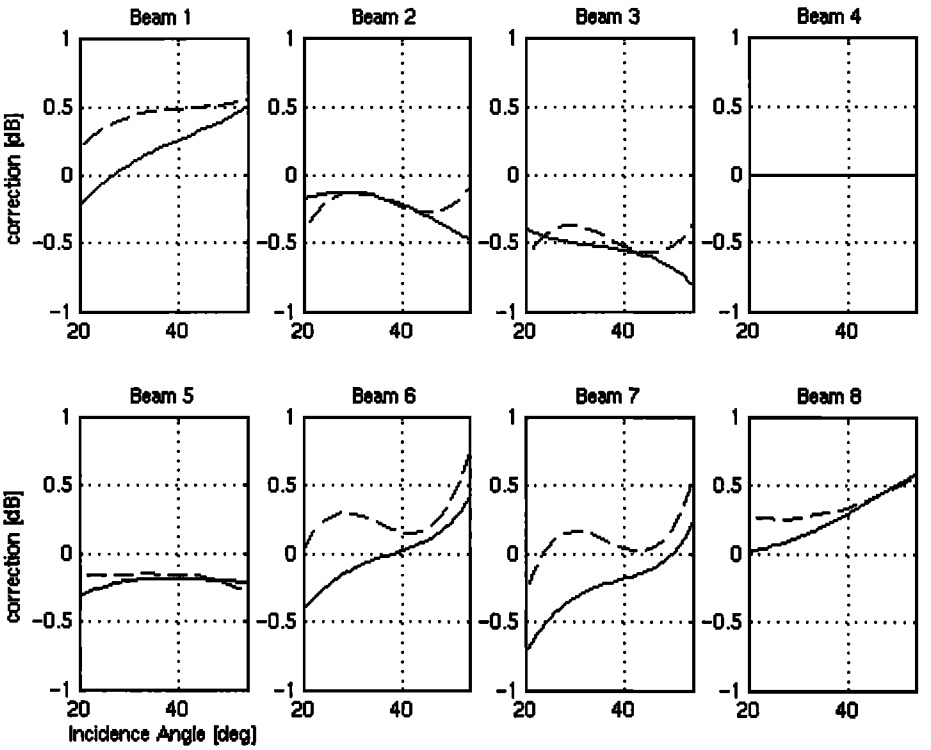

Figure 15. Comparison of NSCAT baseline, ocean-derived, and land-derived beam corrections for descending passes.

rect winds if the GMF were imperfect. Despite this concern the NSCAT engineering team accepted the ocean-based beam corrections because they resulted the best agreement with modeled wind fields over ocean.

The beam balance method proposed herein does not require external information such as modeled wind fields, and our results do not depend on the accuracy of the applied GMF. Our method relies exclusively on the NSCAT σ^0 data. It is recommended that users of NSCAT σ^0 data remove ocean-based corrections and apply our beam balance defined in (4), particularly for land applications.

Comparisons of the ocean and land beam corrections are illustrated in Figure 14 (ascending passes) and Figure 15 (descending passes). Note that ocean beam corrections use beam 4 for normalization of the other beams. For comparison purposes the land beam corrections are also presented as normalized values to beam 4.

6. Conclusions

A simple method is applied to remove NSCAT σ^0 measurement biases caused primarily by errors in measured antenna gains. This method uses homogeneous, isotropic, wide-area land targets to provide relative antenna gain corrections. The advantage of the method is its simplicity and its relatively fast convergence. A 3-week time period is adopted as a compromise between the amount of accumulated data and seasonal effects in target's response. The method adjusts all antennas to the reference value of the normalized radar cross section that is, for each incidence angle θ, the average σ^0 from all beams. The corrections are calculated for each antenna beam as differences between the measurements and the reference $\sigma^0(\theta)$ response. The magnitude of the resulting corrections (up to 1 dB) clearly demonstrates the necessity of the on-orbit calibration before producing the final NSCAT σ^0 data set. Comparisons are made with independent beam corrections from analyzes of global ocean backscatter. Small differences exist as a function of incidence angle for the various beams; but they are generally less than 0.2 dB. When either set of beam biases is used for NSCAT wind retrievals, the results are nearly identical. This justifies the decision to use ocean-derived beam biases to produce ocean winds.

For applications of NSCAT raw σ^0, it is suggested that the ocean-derived beam biases be removed and the beam corrections reported herein be applied. To aid this process, a table of differential corrections is available from the Jet Propulsion Laboratory, Physical Oceanography Distributed Active Archive Center (PO-DAAC).

Acknowledgments. This work was sponsored under contract to the NSCAT project of the Jet Propulsion Laboratory. The authors wish to thank Jay Wilson of Brigham Young University for the generation of Amazon and Siberian masks used in this work.

References

Birer, I. J., E. M. Bracalente, G. J. Dome, J. Sweet, and G. Berthold, σ^0 signature of the Amazon rain forest obtained from the Seasat Scatterometer, *IEEE Trans. Geosci. Remote Sens., GE-20*, 11-17, 1982.

Freilich, M. H., and R. S. Dunbar, The accuracy of the NSCAT 1 vector winds: Comparisons with National Data Buoy Center buoy, *J. Geophys. Res.*, this issue.

Kennet, R. G., and F. K. Li, Seasat over-land scatterometer data, 2, Selection of extended area land target sites for the calibration of spaceborne scatterometers, *IEEE Trans. Geosci. Remote Sens., GE-27*, 779-788, 1989.

Long, D. G., and G. B. Skouson, Calibration of spaceborne scatterometers using tropical rain forests, *IEEE Trans. Geosci. Remote Sens., 34*, 413-424, 1996.

Long, D. G., P. Hardin, and P. Whiting, Resolution enhancement of spaceborne scatterometer data, *IEEE Trans. Geosci. Remote Sens.*, *31*, 700-715, 1993.

Naderi, F., M. H. Freilich, and D. G. Long, Spaceborne radar measurement of wind velocity over the ocean - An overview of the NSCAT scatterometer system, *Proc. IEEE*, *79*, 850-866, 1991.

Schroeder, L. C., D. H. Boggs, G. Dome, I. M. Halberstam, W. L. Jones, W. J. Pierson, and F. J. Wentz, The relationship between wind vector and normalize radar cross section used to derive Seasat A satellite scatterometer winds, *J. Geophys. Res.*, *87*, 3318 - 3336, 1982.

Wentz, F. J., and D. Smith, A model function for the ocean normalized radar cross section at 14 GHz derived from NSCAT observations, *J. Geophys. Res.*, this issue.

Wilson, C. J., Calibration of an attitude estimation for a space-borne scatterometer using measurements over land, M. S. thesis, Brigham Young Univ., Provo, Utah, 1998.

W. L. Jones and J. Zec, Central Florida Remote Sensing Laboratory, Electrical and Computer Engineering Department, University of Central Florida, Orlando, FL 32816. (e-mail: ljones@pegasus.cc.ucf.edu; josko@bruce.engr.ucf.edu.)

D. G. Long, Electrical and Computer Engineering Department, Brigham Young University, Provo, UT 84601.

(Received February 25, 1998; revised October 6, 1998;
accepted November 16, 1998.)